KINETICS OF DEHYDRATION OF 1-BUTANOL OVER ZEOLITES

O. OLAOFE[a] and P. L. YUE[b]

[a] *Department of Food Technology, Federal Polytechnic, Ado-Ekiti, Nigeria and*
[b] *School of Chemical Engineering, Bath University, Great Britain*

Received September 17th, 1984

The kinetics of catalytic dehydration of 1-butanol have been studied on three commercial types of zeolites varied in cage structures, pore sizes, and acidity at 200—300°C. The dehydration reactions were performed in a continuous stirred gas–solid reactor. Butenes and dibutyl ether were the principal products. Both simple power-law and Hougen–Watson types of rate expressions have been used to model the dehydration reactions kinetics. The former satisfactorily correlates the kinetic data procured over all the zeolites except in the case of dibutyl ether formation over ZNa. The Hougen–Watson type of rate expression adequately fitted the rate of formation of both products. The reaction orders with respect to 1-butanol were approximately equal to zero. The kinetic and adsorption parameters were evaluated and satisfactorily correlated as functions of reaction temperature. Activation energies for the formation of dibutyl ether over zeolites ZNa and 4A are affected by pore diffusion.

Most kinetic studies on 1-butanol dehydration (Table I) have been performed over alumina. 1-Butanol has been found to dehydrate primarily to form olefin and/or ether depending on the reaction conditions. The values of activation energy deduced from the data in the literature vary quite widely. The majority of experimental work reported in the literature[1–5] covers a range of fairly low partial pressures of 1-butanol, except[4] which covers high pressure between 0·10 to 0·78 MPa.

However, there are considerable experimental data in the literature on the catalytic dehydration of other alcohols[6–10]. The reaction route still remains a controversial subject. There are three main reaction routes: *a*) Consecutive, *b*) parallel, and *c*) combination of *a*) and *b*) called consecutive-simultaneous reaction scheme. There is more evidence supporting the parallel scheme than the consecutive. This has been fully discussed by Yue and Olaofe[11]. The consecutive-simultaneous reaction scheme could be reduced to *b*) as explained by Yue and Olaofe[11]. Both simple power-law (PL) and Hougen–Watson (HW) types of rate models have been used in the literature to represent kinetic data on the catalytic dehydration of 1-butanol (Table I). The order of the reactions for both the formations of olefin and ether varied between zero and one. At low concentration, the apparent order of reaction was usually found to be one and tends to zero at high concentration. From the kinetic modelling point of view, it would be useful to extend the study of the reactions to cover both low and high pressure range. Authors who used the HW type of rate equations have mostly assumed that surface reaction is the rate controlling step. For the olefin formation, rate expression based on dual-site and single-site mechanisms have been proposed and tested by some authors[4,5].

The present study is concerned with the kinetics of catalytic dehydration of 1-butanol on three types of zeolites varied in cage structure, pore sizes, and acidity in the temperature range 200–300°C.

EXPERIMENTAL

Three commercial zeolites — Laporte 13X and 4A Zeolites and Norton Zeolon, ZNa, have been used as catalysts. Their physical and chemical properties are summarised in Table II. The Laporte Zeolites are spherical beads while the Norton Zeolon is in the form of cylindrical extrudate.

The dehydration reactions were performed in a continuous stirred gas–solid reactor (CSGSR) similar to that discussed by Brisk and coworkers[12]. Figure 1 shows the schematic diagram of the experimental equipment.

High purity nitrogen was used as a reactant diluent. It was passed through a column containing 13X zeolite to remove any moisture present. Gas chromatographic analysis of the nitrogen feed showed no detectable impurities. 1-Butanol of purity higher than 99·5% was delivered by a metering pump to an evaporation unit, where it was mixed with the nitrogen diluent. The mixed feed was brought to nearly the chosen reaction temperature in the electrically heated furnace. Connecting tubes were kept at high enough temperatures by heating tapes to avoid the condensation of materials. Alcohol flow rate was measured by a burette attached to the feed tank. The nitrogen supply was regulated by a mass flow rate control valve. Its flow rate was measured by a bubble flowmeter downstream of the reactor after the removal of the condensable materials.

The reactor chamber temperature was measured by a chromel/alumel thermocouple. Heat transfer calculations gave an estimate of less than 1°C difference between chamber and the catalyst temperature. Reactor pressure was kept at 0·1 MPa.

Reactor effluent was analysed by a gas chromatograph. A glass column of 1 m length and 4·0 mm internal diameter packed with Porapak Q was used for the resolution of the products, while the resolution of the isomeric butenes was achieved in a glass column of 7·3 m length and 3·2 mm internal diameter packed with 20% bis(2-methoxyethyl) adipate on Chromosorb P-AW kept at 40°C (ref.[13,14]). Calibration curves for the different components were prepared. Mean values of the measurements were obtained from three or more reproducible analyses. The experimental error gave a deviation of no more than 4% from the mean for each component. A subsequent paper will deal with the butenes product distribution.

TABLE I
Published data on catalytic dehydration of 1-butanol

Catalyst	Product	T, °C	P_A, MPa	Model	Reaction Order	E_A/E_E kJ g mol^{-1}	Ref.
Zeolite X	O	228	low	PL	1	126	2
Zeolite Y	O	256	low	PL	1	113	2
γ-Alumina	O, E	238–328	0·06	PL	0	129	3
Silica	O	205–307	0·10–0·78	HW	—	—	4
Alumina	O	400	0·1–50	HW	—	—	5
Alumina	O	350, 410	—	—	—	—	6

TABLE II

Physical and chemical properties of zeolites used

Properties	13X	4A	ZNa
Chemical formula or structure	$Na_{41}Al_{41}Si_{106}O_{294}.264\ H_2O$	$Na_{12}Al_{12}Si_{24}O_{48}.27\ H_2O$	$Na_8Al_8Si_{40}SO_{96}.24\ H_2O$
SiO_2/Al_2O_3	2·6	2·0	10·0
Nominal aperture size (nm)	1·00	0·42	0·57 × 0·70
BET surface area (m^2g^{-1})	359	10	103
Bulk density (kg m^{-3})	670	740	680
Particle size (mm)	1·0—2·0	1·0—2·0	1·588 by 8·5
Binder	natural clay	natural clay	self binding
Percentage of binder	15—20	15—20	—
Crystalline structure	body centre cubic	simple cubic	—
Physical form	spherical beads	spherical beads	1·588 mm extrudates

True surface reaction rates can be obtained only if the experiments have been performed under conditions which are not limited by diffusional processes. At high gas velocities, interphase mass transfer will not be rate-limiting. The spinning speed was therefore varied to establish the conditions when the rates were not controlled by interphase diffusion. It was observed that at the speed of 2 000 min^{-1}, reaction rates are unaffected by external mass transfer, which agrees with the conclusions of others[15,16]. Experiments with different particle sizes can determine the influence of molecular and Knudsen diffusion. The reactor used in the present study does not permit the use of fine catalyst particles. Secondly, the study of diffusional processes within zeolite crystals are not fully understood as yet, because, other modes of diffusion in zeolites crystalline have been reported[17]. In this paper, possible influence of pore diffusion on the present results will be noted whenever appropriate.

Reaction temperature range 200—300°C was chosen for 1-butanol dehydration. The 1-butanol feed rate was varied to achieve a wide range of alcohol partial pressures at constant total pressure. At least five partial pressures of alcohol were used for a given reaction temperature and a zeolite.

RESULTS AND DISCUSSION

The dehydration of 1-butanol over zeolites 13X, 4A, and ZNa yielded two principal products, the ether and the olefins. The gas chromatograph analysis showed the

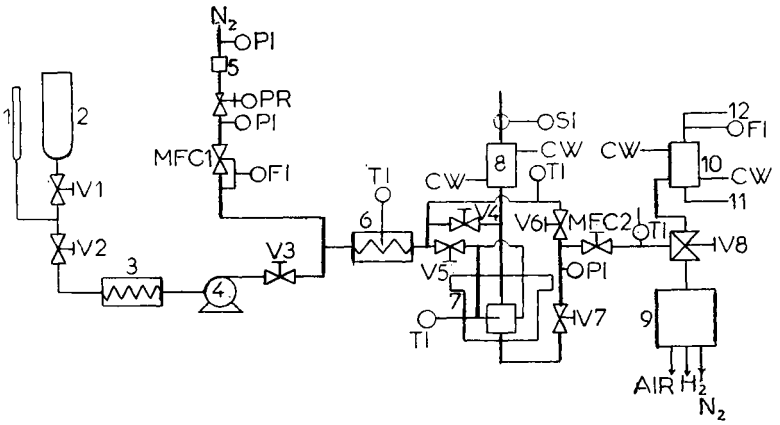

FIG. 1

Schematic diagram of the experimental equipment. 1 Burrete (1 ml), 2 feed tank (1 l), 3 cooler, 4 metering pump (Metering pump L + d), 6 molecular sieve 13X column, 5 preheater, 7 spinning basket reactor, (Imperial Chemical Industry), 8 spinning drive unit, 9 gas–liquid chromatograph, (Pye Unicam), equipped with both FID detector and amplifier, 10 condenser, 11 condensate, 12 gaseous effluent, V1—V8 valves, TI temperature indicator, PI pressure indicator, SI speed indicator, CW cooling water, PR pressure regulator, MFC mass flowrate regulator, FI flowrate indicator

formation of small quantities of butylaldehyde which is a product of the dehydrogenation catalysed e.g. by copper or nickel[18]. Experiments without zeolites in the reactor confirmed the formation of aldehydes catalysed by the copper and nickel present in the tubings and reactor walls. The dehydration reactions, however, are not affected by these metals. The rates of formation of butenes and dibutyl ether were calculated based on material balance which had taken the side products into account.

Since the zeolites were found to deactivate with time, their activity was measured regularly. It was found that when fresh catalysts were used, the catalytic activity always dropped rapidly in the initial stage of the experiments and then levelled off for a considerable time. The present kinetic data were obtained in the period of constant activity and the results were reproducible to within 10%.

All the kinetic data have been modelled according to both power-law kinetic and Hougen-Watson type of kinetic expressions. The latter approach is based on the classical Langmuir–Hinshelwood mechanism, with surface reaction or adsorption – desorption of reactants and/or products assumed to be rate controlling[11]. Preliminary discrimination of all plausible rate expressions was conducted to eliminate some of the less probable models. For example: *a*) The absorption–desorption equilibrium constants of ether and olefin have been found to be very small, hence the desorption of these two species cannot be rate limiting. *b*) The partial pressures of ether, olefin, and water in the present experiments were very low compared with that of 1-butanol, thus the products $K_E P_E$, $K_O P_O$, and $K_H P_H$ were much smaller than $K_A P_A$. *c*) The adsorption of nitrogen (diluent) on zeolites is not appreciable above 244 K (ref.[19,20]).

Thus we can conclude that $K_A P_A$ is the major contribution to the adsorption term in the Hougen–Watson model. For the olefin formation reaction, the equilibrium constant is high and the reaction can be considered irreversible.

Parameters in the remaining models were estimated accordingly to the methods proposed by Kittrell[21]. Both multilinear and nonlinear regression analyses were applied to the experimental data. Results from the linear regression were used as first estimates for nonlinear regression. The theoretical aspects of parameter estimation and regression techniques are well established[22,23] and details of the computer programs have been given by Dixon and Brown[24].

Formation of Butenes

Figs 2–4 illustrate the effect of partial pressure of 1-butanol on the rate of formation of butenes. The rates of formation of butenes are almost independent of the partial pressure of alcohol, indicating that the reactions tend towards zero order in 1-butanol in terms of power law kinetics. At low temperature, the reactions are approximately zero order. This is because chemisorption decreases with increasing temperature. The reaction order with respect to 1-butanol slightly increases with increasing temperature. However, of all the power-law rate expressions tested, the most successfuly one

was

$$r_0 = A_0 \exp\left(-E_0/RT\right) P_A^n . \qquad (1)$$

Table III gives the best estimates of the constants for expression (*1*), together with the statistical properties (*t*-ratio, *F*-ratio, and *R*-squared coefficient). A high *t*-ratio means small standard deviation, hence a higher confidence level. The calculated *F*-ratio gives an indication of the significance of the regression, while the

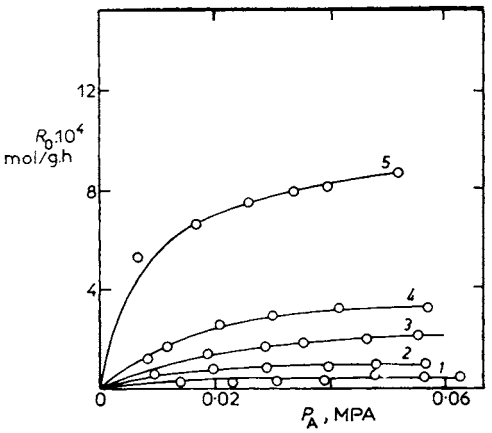

FIG. 2

The influence of the partial pressure of 1-butanol on the rate of formation of butene over Zeolite 13X. *1* 228, *2* 241, *3* 252, *4* 258, *5* 272°C

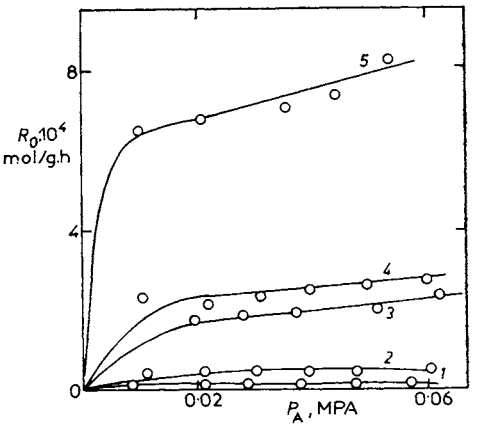

FIG. 3

The influence of the partial pressure of 1-butanol on the rate of formation of butene over Zeolite 4A. *1* 231, *2* 250, *3* 271, *4* 278, *5* 297°C

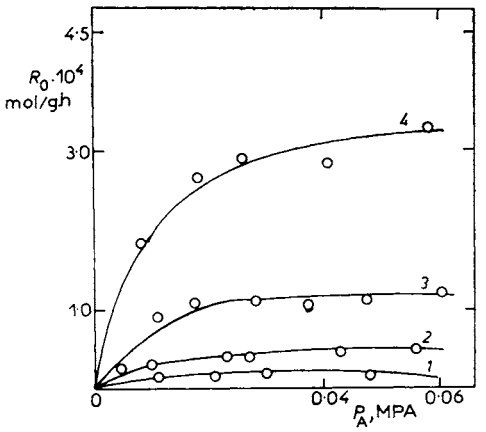

FIG. 4

The influence of the partial pressure of 1-butanol on the rate of formation of butene over Zeolite ZNa. *1* 235, *2* 255, *3* 275, *4* 300°C

last column shows the observed F-ratio at 95% confidence level. If the observed F-ratio exceeds the critical F-ratio at 95% confidence level by a factor of four, statistically significant regression is said to have been achieved. The R-squared gives a measure of how well the regression fits the experimental data. The results in Table III show that the regression of the rate data for butenes formation according to the power-law kinetics are statistically satisfactory over all the zeolites. Butene formation on all the zeolites are close to zero order. The found activation energy for the butenes formation reaction agrees very well with those reported in literature (Table I). The low reaction orders suggest that the active sites of the catalyst are nearly saturated with the alcohol and also implies the absence of external mass transfer effect.

A compensation effect is shown by the zeolites on the dehydration of 1-butanol to the butenes. A good straight line between the logarithms of the preexponential factor and the activation energy was obtained. The equation for the line is given by

$$\ln A_O = -12{\cdot}0 + 0{\cdot}25E_O \,. \qquad (2)$$

The agreement between the present results (reaction order and activation energy) and literature values is rather remarkable in view of the different treatment of the kinetic data and different experimental conditions used here. This agreement suggests that the reaction mechanisms and the rate determining step are probably the same for the butenes formation over a wide range of reaction temperature and different catalysts.

The two Hougen–Watson expressions derived for the formation of butenes, based on the assumption that the surface reaction is rate-limiting, are the so-called dual-site and single site mechanism models (Eqs (*3*) and (*4*))

$$r_O = \frac{k_O K_A P_A}{(1 + K_A P_A)^2} \qquad (3)$$

TABLE III

Kinetic parameters for power-law model: butenes formation

Zeolite	13X	4A	ZNa
A_o, kmol kg^{-1} h^{-1} MPa^{-n}	$7{\cdot}3 \cdot 10^{11}$	$4{\cdot}3 \cdot 10^{10}$	$5{\cdot}4 \cdot 10^{5}$
E_0, kJ mol^{-1}	159	151	105
n	0·28	0·12	0·17
t-ratio	8·0	4·1	4·9
R^2	99	99	99
F-ratio critical (95%)	20	20	20
observed	1 200	770	3 000

$$r_O = \frac{k_O K_A P_A}{(1 + K_A P_A)} . \qquad (4)$$

Expression (*3*) qualitatively predicts reaction order between 1 and -1 in alcohol while expression (*4*) allows for a reaction order less or equal to one. Both expressions allow for the depressive behaviour of alcohol. Effects of the weakly adsorbed species and those present in relatively small concentrations have been neglected.

Both correlations (*3*) and (*4*) show high *R*-squared coefficients for all zeolites at all reaction temperatures. However, the kinetic data over ZNa catalyst when fitted to the single-site model (SR1) resulted in a negative adsorption coefficient at 235°C.

The single-site model for ZNa should have been therefore rejected because of this negative adsorption coefficient, however, the non-linear analysis was still performed. Nonlinear regression confirmed that the single site model was not appropriate for this set of kinetic data because an unlikely high adsorption equilibrium constant was obtained (Table IV). It can therefore be concluded that the SR1 model fails to correlate satisfactorily the butenes data over ZNa. In the nonlinear analysis, the sum of squares of residuals (SSR) for the SR1 and SR2 models are very small. This suggests that satisfactory correlations are achieved. The results of the nonlinear regressions are shown in Table IV and a comparison of the linear and nonlinear regressions is shown in Table V. There is an excellent agreement between the parameters obtained from both techniques which strongly suggests that the kinetic data are good[25].

The temperature dependence of the kinetic and adsorption parameters is illustrated in Fig. 5. The graph is in a good agreement with the Arrhenius law suggesting that the kinetic data were procured in the surface reaction rate controlling regime and with no significant catalyst deactivation. The temperature dependence of the adsorption equilibrium constants follows the van't Hoff type of equation. The adsorption plot for the zeolites 4A and ZNa shows a positive slope, which suggests that adsorption of 1-butanol on these catalysts is exothermic. However, on zeolite 13X, the adsorption plot has negative slope, showing that the 1-butanol process is endothermic and dissociative.

The estimated preexponential factors, activation energies, enthalpies of the desorption of 1-butanol obtained by linear analysis are presented in Table VI. The activation energies from the HW models agree quite well with those obtained from the power law models (Table III). This indicates that the adsorption process has no significant effect on the apparent activation energies of the dehydration of 1-butanol, probably due to the low reaction orders. The apparent activation energies show no discernible effect of either external or pore diffusion. It should, however, be cautioned that diffusion limitations might manifest in the formation of dibutyl ether.

Formation of Dibutyl Ether

Typical kinetic rate data are shown in Fig. 6. The power law model is, in most cases, satisfactory in representing the kinetics of butenes formation. In the dehydra-

TABLE IV
Parameters for Hougen–Watson models

Zeolite	Model	T, °C	$k_0 \cdot 10^4$ kmol kg^{-1} h^{-1}	SD . 10^4	K_A MPa^{-1}	SD	SSR . 10^{10}
13X	SR2	228	1·9	0·28	13	0·62	1·0
		241	4·0	0·16	22	0·34	1·0
		252	8·0	0·43	20	0·39	3·0
		258	13	0·32	116	0·12	1·0
		272	33	1·4	27	0·48	52
13X	SR1	228	0·59	0·15	63	1·2	1·0
		241	1·2	0·04	120	2·0	0·5
		252	2·4	0·15	110	2·6	1·0
		258	4·4	0·37	63	1·7	3·0
		272	9·4	0·30	170	2·7	8·0
4A	SR2	232	0·55	0·03	33	0·72	0·5
		250	2·0	0·07	31	0·47	0·5
		271	9·0	0·55	27	0·65	9·0
		278	11	0·40	27	0·42	5·0
		297	32	1·8	27	0·61	104
4A	SR1	232	0·14	0·01	460	25	0·5
		250	0·49	0·01	440	13	0·6
		271	2·4	0·01	280	11	2·0
		278	2·9	0·07	240	4·0	0·5
		297	8·4	0·47	290	13	29
ZNa	SR2	235	0·80	0·03	45	0·49	0·5
		255	1·9	0·12	30	0·66	0·5
		275	4·7	0·15	29	0·37	1·0
		300	13	0·56	25	0·38	6·0
ZNa	SR1	235	0·18	0·01	17 . 10^3	0	0·5
		255	0·51	0·02	230	5·0	0·5
		275	1·2	0·04	300	8·3	0·5
		300	3·6	0·20	140	3·4	2·0

tion of 1-butanol to dibutyl ether, the power law rate expression is satisfactory for zeolites 13X and 4A, however not for zeolite ZNa. The estimated parameters

$$r_E = A_E \exp(-E_E/RT)\, P_A^m \qquad (5)$$

and the statistical properties are presented in Table VII. The reaction order for the formation of dibutyl ether lies between zero and half order. This result is in general agreement with literature values (Table I). The reaction orders for the dibutyl ether formation are higher than for butene formation.

The activation energies for the formation of dibutyl ether are shown in Table VII; these values are low with the exception of the activation energy for the formation of dibutyl ether over 13X. This is probably due to the influence of pore diffusion.

TABLE V

Comparison between linear and nonlinear regression: 1-butanol over 13X Zeolite

Temperature, °C	228	241	252	258	272
		Model SR 2			
Linear regression					
$k_O \cdot 10^4$ [a]	1·8	4·0	8·0	13·0	34·0
K_A [b]	14	22	21	16	29
Nonlinear regression					
$k_O \cdot 10^4$ [a]	1·9	4·0	8·0	13	33
K_A [b]	13	22	20	16	27
		Model SR 1			
Linear regression					
$k_O \cdot 10^4$ [a]	0·61	1·1	2·5	4·3	9·6
K_A [b]	52	110	89	68	160
Nonlinear regression					
$k_O \cdot 10^4$ [a]	0·59	1·2	2·4	4·4	9·4
k_A [b]	63	120	110	63	170

[a] kmol kg^{-1} h^{-1}; [b] MPa^{-1}.

The rate data on dibutyl ether formation have also been fitted with the Hougen–Watson type kinetic expressions. Many rate equations can be derived[13] but only three models, which assume that the bimolecular surface catalysed reaction is the rate controlling step, will be presented here: *a*) The Langmuir–Hinshelwood mechanism (LHM) model assumes that the surface reaction may take place in which two

TABLE VI

Kinetic and adsorption parameters for Hougen–Watson models

Zeolite	Model	A_O kmol kg^{-1} h^{-1}	E_O kJ kmol^{-1}	ΔH_A kJ kmol^{-1}
13X	SR2	$6{\cdot}1 \cdot 10^{11}$	150	26
	SR1	$1{\cdot}1 \cdot 10^{11}$	146	33
4A	SR2	$2{\cdot}3 \cdot 10^{11}$	150	− 8
	SR1	$8{\cdot}5 \cdot 10^{10}$	154	− 24
ZNa	SR2	$3{\cdot}1 \cdot 10^{6}$	104	− 21
	SR1	4·7	113	−146

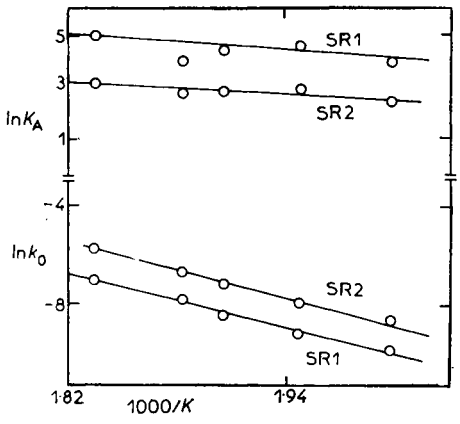

FIG. 5

Temperature dependence of the kinetic and adsorption thermodynamic equilibrium constants. The dehydration of 1-butanol to butene over zeolite 13X

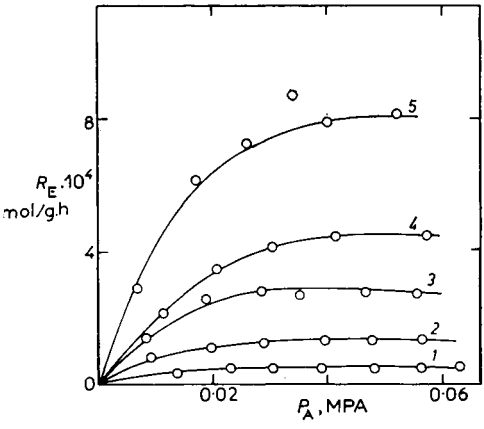

FIG. 6

The influence of the partial pressure of 1-butanol on rate of formation of di-1-butyl ether over Zeolite 13X. *1* 228, *2* 241, *3* 252, *4* 258, *5* 272°C

adjacently chemisorbed 1-butanol molecules react to form the chemisorbed products. The rate of formation of dibutyl ether is given by

$$r_e = \frac{k_E K_A^2 (P_A^2 - P_W P_E / K_{eq})}{(1 + K_A P_A)^2} . \tag{6}$$

b) The Rideal–Eley mechanism (REM1) assumes that the surface reaction may occur in which one 1-butanol molecule from the gas phase reacts directly with another chemisorbed 1-butanol molecule in the presence of a vacant site adjacent to the chemisorbed products. The rate of formation of dibutyl ether is

$$r_E = \frac{k_E K_A (P_A^2 - P_W P_E / K_{eq})}{(1 + K_A P_A)^2} . \tag{7}$$

c) The REM2 model assumes that the surface reaction may take place by a Rideal–Eley mechanism as defined in *b*), but not in the presence of an adjacent vacant site and only the product water is chemisorbed while the product ether goes directly into the gaseous phase. The rate of formation of the ether is represented by

$$r_E = \frac{k_E K_A (P_A^2 - P_E P_W / K_{eq})}{(1 + K_A P_A)} . \tag{8}$$

Qualitatively, the first two models predict the order of reaction between 0 and 2, while the third model predicts the order of reaction between 1 and 2. All models

TABLE VII

Kinetic parameters for power-law model: ether formation

Zeolite	13X	4A	ZNa
A_E, kmol kg^{-1} h^{-1} MPa^{-m}	$1{\cdot}7 \cdot 10^{10}$	$8{\cdot}7 \cdot 10^{2}$	1·3
E_E, kJ mol^{-1}	142	84	54
m	0·38	0·29	0·56
t-ratio	5·8	5·7	4·8
R^2	95	95	79
F-ratio critical (95%)	20	19	19
observed	280	88	17

predict the depressive behaviour of 1-butanol but the influence is stronger with the first two models. The models also include the influence of reverse reaction (Table VIII).

Both linear and nonlinear regression analyses were performed. In both cases the results obtained from the linear method were confirmed by nonlinear technique. The results obtained by nonlinear method are presented in Table V. The correlations showed very high R^2 coefficients and low SSR value, which indicates that satisfactory correlations were obtained.

With the REM2 model, the adsorption–desorption equilibrium constants were often found to be either very high with nonlinear technique or negative with linear method at all reaction temperatures. A negative adsorption coefficient is physically meaningless but has sometimes been ascribed to enhanced adsorption. The concept has not been widely accepted, thus the last model is rejected. Both the LHM and REM1 models gave reasonable values of adsorption coefficients.

Fig. 7 shows the temperature dependence of the kinetic and adsorption equilibrium constants. The plots follow the Arrhenius and van't Hoff equations, respectively. The apparent activation energy preexponential factors and heat of adsorption are presented in Table IX. The activation energies from LHM and REM1 models compare well with those obtained from the power-law model. The heat of adsorption shows an exothermic adsorption process.

It is not appropriate to distinguish between LHM and REM1 models by using the kinetic data. Mathematically, the two models have the same form and only differ in the parameter K_E. The apparent activation energies and preexponential factor obtained from the two models should be related to each other as given by the fol-

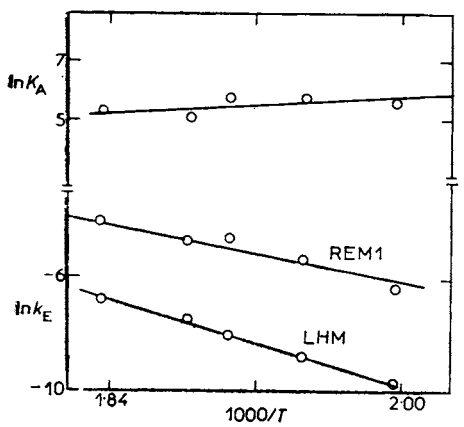

FIG. 7

Temperature dependence of the kinetic and adsorption equilibrium constants. The dehydration of 1-butanol to di-1-butyl ether over 13X zeolite. From top to bottom: K_a, REM 1, LHM

lowing equations.

$$E_E\,(\mathrm{LHM}) = E_E\,(\mathrm{REMI}) + \Delta H_A \qquad (9)$$

$$A_{O_{LHM}} = A_{O_{REMI}}/K_{AO} \qquad (10)$$

TABLE VIII
Parameters for Hougen–Watson models

Zeolite	Model	T, °C	$k_E \cdot 10^4$ kmol kg^{-1} h^{-1}	SD . 10^4	K_E MPa^{-1}	SD	SSR . 10^{10}
13X	LHM	228	0·63	0·03	280	6·0	0·5
		241	1·5	0·04	310	3·0	0·5
		252	3·4	0·21	300	8·0	4·0
		258	15·9	0·43	150	3·2	6·0
		272	11	0·77	180	4·0	29
13X	REM1	228	17	3·0	280	0·0	0·5
		241	48	3·9	310	3·0	0·5
		252	99	22	300	8·0	4·0
		258	90	12	150	3·0	6·0
		272	200	30	180	4·0	29
13X	REM2	228	1·1	0·15	$60 \cdot 10^3$	0	3·0
		241	3·2	0·46	$35 \cdot 10^4$	0	18
		252	6·9	1·1	$76 \cdot 10^4$	0	95
		258	10	1·5	$76 \cdot 10^3$	0	150
		272	21	2·7	$49 \cdot 10^3$	0	460

TABLE IX
Kinetic and adsorption parameters for Hougen–Watson models

Zeolite	Model	$K_E \cdot 10^4$ kJ mol^{-1}	E_E kJ kmol^{-1}	ΔH_A kJ mol^{-1}
13X	LHM	$2{\cdot}6 \cdot 10^{11}$	151	−29
	REM1	$8{\cdot}3 \cdot 10^9$	121	—

The present results clearly support this relationship. For example, E_E (LHM) have the value 151 kJ kmol^{-1}, which is practically equal to the sum of E_E(REM1), 121 kJ kmol^{-1} and absolute value of ΔH_A (if adsorption is exothermic) which is -29 kJ kmol^{-1}.

The 1-butanol thermodynamic equilibrium constant for the formation of dibutyl ether is found to be greater than that for the formation of butene under the same reaction conditions. The observation suggests that 1-butanol dehydration reactions for dibutyl ether and butenes do not take place on the same active site. Furthermore, it indicates that the saturation partial pressure of 1-butanol is higher for dibutyl ether formation than for butenes formation. This is also evident in the difference in reaction orders as has been discussed previously.

CONCLUSIONS

Empirical power functions rate expressions satisfactorily correlated the kinetic data on the dehydration of 1-butanol to dibutyl ether and butenes over zeolites 13X, 4A, and ZNa. The butenes formation has an approximately zero reaction order while the dibutyl ether formation order vary between zero and half.

For the formation of butenes, the Hougen–Watson type of rate expressions based on dual site mechanism (SR 2) and single site mechanism (SR1) successfully fitted the kinetic data over all zeolites, however, the SR1 model fails over ZNa zeolite. For the dibutyl ether formation, LHM and REM1 models adequately correlated the rate data well.

Activation energies for the formation of butenes from the power law and Hougen–Watson type of rate expression show not discernible effect of pore diffusion in the temperature range investigated. However, the influence of pore diffusion is seen in the results of dibutyl ether formation on zeolites 4A and ZNa. Models LHM and REM1 remain indistinguishable.

Adsorption–desorption equilibrium constants obtained from the Hougen–Watson type of rate equation satisfactorily follow van't Hoff type of expression.

The dehydration of 1-butanol can be considered to follow a simultaneous reaction scheme and found to require different active sites. Both reactions proceed through different reaction routes.

LIST OF SYMBOLS

A_j preexponential factor for the formation of j in power-law models (kmol kg^{-1} kg^{-1} . h^{-1} MPa^{-n})

E_j activation energy for the formation of j (kJ gmol^{-1})

ΔH_A heat of adsorption (kJ gmol^{-1})

k_j kinetic parameter in HW models for the formation of j (kmol kg^{-1} h^{-1})

K_j adsorption-desorption equilibrium constant for j (MPa^{-1})

K_{eq} chemical equilibrium constant for the reversible ether formation reaction (—)
m, n reaction order in equations (*4*) and (*1*)
P_j partial pressure of j (MPa)
r_j rate of formation of (kmol kg^{-1} h^{-1})
T absolute temperature (K)

Subscripts

A alcohol
E ether
O olefin
W Water

Abbreviations

HW Hougen–Watson type of rate expression
LHM Langmuir–Hinshelwood mechanism
PL power-law
REM1 Rideal–Eley mechanism based on dual site
REM2 Rideal–Eley mechanism based on single site
SR1 surface reaction mechanism based on dual site
SR2 surface reaction mechanism based on single site
SSR sum of squares of residuals
SD standard deviation

REFERENCES

1. Pines H., Haag W. D.: J. Amer. Chem. Soc. *82*, 2471 (1960).
2. Gryaznova Z. V., Ermilova M. N., Tsitsishvili G. V., Androwiashwili T. G., Krupennikova Yu. A.: Kinet. Katal. *10*, 1099 (1969).
3. Stauffer J. E., Kranich W. L.: Ind. Eng. Chem. Fundam. *1*, 107 (1962).
4. Miller D. N., Kirk R. S.: AIChE J. *8*, 183 (1962).
5. Maurer J. F., Sliepcevich C. M.: AIChE Symp. *48*, 31 (1952).
6. Butler J. D., Poles T. C., Wood B. T.: J. Catal. *16*, 239 (1970).
7. Gentry S. J., Agudo A. L.: J. Chem. Soc., Faraday Trans. 1, *70*, 1685 (1970).
8. Stone F. S., Agudo A. L.: Z. Phys. Chem. (Wiesbaden) *64*, 161 (1969).
9. Topchieva K. V., Tkhoang H. S.: Kinet. Katal. *14*, 1491 (1973).
10. Gottifredi J. C., Yeraman A. A., Cunningham R. E.: J. Catal. *12*, 245 (1968).
11. Yue P. L., Olaofe O.: Ind. Chem. Eng., Prod. Res. Develop. *62*, 81 (1984).
12. Brisk M. L., Day R. L., Jones M., Warren M. A.: Trans. Inst. Chem. Eng. *46*, T3 (1968).
13. Olaofe O.: *Thesis*. University of Bath 1982.
14. Mindcup R.: J. Chromatogr. Sci. *16*, 380 (1978).
15. Ford F. R., Perlmutter D. D.: Chem. Eng. Sci. *19*, 371 (1964).
16. Santacesaria E., Morbidelli M., Carrá S.: Chem. Eng. Sci. *38*, 909 (1981).
17. Ruthen D. M., Derrah R. I., Loughlin K. F.: Can. J. Chem. Eng. *51*, 3514 (1973).
18. Jain J. R., Pillai C. N.: J. Catal. *9*, 322 (1970).
19. Hougen O. A., Watson K. M.: *Chemical Engineering Principles*, Part 3. Wiley, New York 1947.
20. Hersh C. K.: *Molecular Sieves*. Reinhold, New York 1961.

21. Kitrell J. R.: Advan. Chem. Eng. *8*, 97 (1970).
22. Kitrell J. R., Mezaki R., Watson C. C.: Ind. Eng. Chem. *57* (12), 18 (1965).
23. Lapidus L., Peterson T. L.: AIChE J. *11*, 891 (1965).
24. Dixon W. J., Brown M. B.: Biomedical Computer Programs. University of California Press 1979.
25. Draper N. R., Smith H.: *Applied Regression Analysis*. Wiley, New York 1966.